RESEARCH PAPER

Acta Neurobiol Exp 2025, 85: 149–157
DOI: 10.55782/3xhm8m33

Analysis of gene expression and biological processes in the Wallerian degeneration segments of rat distal nerves

Zhengming Wang[1,2&], Yichun He[1,2&], Yushan Guo[1], Tiantian Tang[1], Nan Jiang[1]*

[1] Department of Trauma Center, China-Japan Union Hospital of Jilin University, Changchun, Jilin, China
[2] Department of Neurosurgery, China-Japan Union Hospital of Jilin University, Changchun, Jilin, China
[&] These authors contributed equally to this work and should be considered co-first authors
** Email: jiangn@jlu.edu.cn*

Peripheral nerve injuries occur due to accidents and in manufacturing every day. Unlike the central nervous system, injured peripheral nerves can self-regenerate after injury. The study explored changes in gene expression and related biological processes after peripheral nerve injury and regeneration. Male Sprague-Dawley rats were divided into six groups and underwent sciatic nerve resection followed by recovery for 0, 3, 6, 10, 15, and 20 days; distal sciatic nerve segments were collected for sequencing, real-time quantitative polymerase chain reaction (RT-qPCR), and Western blotting. According to DNA microarray analysis, approximately 5,000 genes were differentially expressed, and six biological processes were identified at different time points after nerve transection, with expression mainly observed in the mid and latter stages after injury. Four genes (UDP glycosyltransferase 8 [*Ugt8*], C-C motif chemokine ligand 2 [*Ccl2*], neuregulin 1 [*Nrg1*], and heme oxygenase-1 [*Hmox1*]) with nerve regeneration-specific function were selected for further verification using RT-qPCR and Western blot. The results demonstrated that genes such as *Ugt8* decreased initially and then peaked at 20 days, whereas *Ccl2* and *Hmox1* both exhibited two peaks at three and 20 days. *Nrg1* showed a gradual increase, peaking around 15 days. The study identified differential gene expression in distal nerve segments during Wallerian degeneration and analyzed the associated dynamic biological changes. The findings provide insights into research on peripheral nerve injury and regeneration, and further studies will involve screening key genes and more detailed investigations.

Key words: Wallerian degeneration, neural regeneration, distal segments, gene microarray, biological processes

INTRODUCTION

Peripheral nerve injuries commonly occur in daily life, due to accidents and in manufacturing workplaces (Mietto et al., 2015). The central nervous system (CNS) has a limited capacity to recover nerve function after injury. In contrast, damaged peripheral nerves can self-regenerate (Sobrido-Camean et al., 2022; Gong et al., 2023), with reinnervation dependent on the intrinsic capacity of peripheral axons and a supportive growth microenvironment (Li et al., 2020). In the distal region, Wallerian degeneration (WD) involves the disintegration of distal axons, followed by the reconnection of new nerve fibers and myelin sheaths from the proximal axon to the distal side (Yao et al., 2013; Krishnan et al., 2024). These two processes are relatively interdependent pathological physiological events during neural recovery (Fledrich et al., 2019).

The process of peripheral nerve injury and regeneration has been mostly studied based on morphology, regenerative capacity, axon survival, metabolism, excitability, transmission function, and sensitivity to multiple extrinsic and intrinsic signals (Fledrich et al., 2019; Cooke et al., 2022). Over the past decade, by analyzing gene expression profiles during peripheral nerve injury and regeneration, DNA microarray chips have provided insights into trends

Received 29 April 2025, accepted 20 November 2025

in gene expression changes (Zhang et al., 2023; Bhunia et al., 2024). Previous DNA microarray studies have reported upregulation and downregulation of genes and biological processes in proximal nerve segments following peripheral nerve injury and regeneration (Li et al., 2013).

Based on this, the study aimed to identify distal gene expression changes following peripheral nerve injury and uncover the biological processes during WD. We used sequencing technology to detect RNA expression patterns in distal sciatic nerves at 0, 3, 6, 10, 15, and 20 days after transection in adult rats. We then used gene ontology (GO) enrichment analysis to identify which biological processes were associated with differential gene expression.

Microarray expression trends were demonstrated by real-time quantitative PCR (RT-qPCR) and Western blot (WB) analysis (Costa-Silva et al., 2017; Lin et al., 2019; Zhang et al., 2019). We selected four genes (UDP glycosyltransferase 8 [*Ugt8*], C-C motif chemokine ligand 2 [*Ccl2*], neuregulin 1 [*Nrg1*], and heme oxygenase-1 [*Hmox1*]) associated with regeneration after peripheral nerve injury to verify the accuracy of the gene chip. *Ugt8* is involved in complex lipid biosynthesis in myelinating oligodendrocytes (Seyednasrollah et al., 2015; Thamizhoviya et al., 2021), *Ccl2* recruits monocytes, memory T cells, and dendritic cells to sites of inflammation caused by either tissue injury or infection (Dommel et al., 2021), *Nrg1* is produced in numerous isoforms by alternative splicing, which allows it to perform a wide variety of functions of the nervous system and the heart (Wang et al., 2022), while *Hmox1* catabolizes free heme, produces carbon monoxide (CO), up-regulatates the expression of the anti-inflammatorys interleukin 10 (IL-10) and interleukin 1 receptor antagonist (IL-1RA) (Consonni et al., 2024).

Our research focused on the early and middle post-injury periods to identify gene expression in the distal nerves (Yao et al., 2012). At the same time, it also revealed the various biological processes that emerged during regeneration after injury. The findings will provide guidance for research on peripheral nerve injury and regeneration and will subsequently be used for gene screening and interventions.

METHODS

Animal models and tissue collection

Fifty-four male Sprague-Dawley (SD) rats (180–220g) were provided by the Experimental Animal Center of Jilin University. All rats were divided into six groups: 0, 3, 6, 10, 15, and 20 days post-sciatic nerve resection (nine per group). Tissue from each group was then analyzed using three assays (microarray, RT-qPCR, and WB). The number of animal samples per assay was three, and no sample pooling was performed. Although the sample size was relatively small, selecting rats from the same batch and with similar body weights ensured homogeneity and maintained sufficiently low variability. All tests were approved by the Administration Committee of Experimental Animals, Jilin University, China (Consent number: SY201911002), and conducted in accordance with "NIH Guidelines for the Care and Use of Laboratory Animals".

Rats were anesthetized intraperitoneally with medetomidine hydrochloride (20 μg/kg) and sodium pentobarbital plus chloral hydrate (30 mg/kg). Under aseptic conditions, an oblique incision was made in the left buttock, the obturator was isolated, and the sciatic nerve was exposed in the left gluteal muscle gap. The sciatic nerve was transected 0.5 cm from the inferior piriformis; the proximal end was folded to prevent reconnection of the severed nerve ends, and the wound was closed. Postoperative analgesia was given by a single intraperitoneal injection of medetomidine hydrochloride (20 μg/kg). Food and water were freely available to the rats after surgery, and their cages were temperature and humidity-controlled and contained sawdust bedding. The day 0 group was euthanized immediately, and the other groups were euthanized at 3, 6, 10, 15, and 20 days after surgery. Neural tissue samples (0.5 cm) from the distal part of the sciatic nerve were collected within five minutes of death.

RNA isolation and microarray experiments

Total RNA was extracted from distal nerve segments using TRIzol reagent (Invitrogen, CA, USA) according to the manufacturer's protocol. RNA amplification, labeling, and purification were performed using the GeneChip® 3'IVT Express Kit (Affymetrix, CA, USA) following the manufacturer's instructions. Hybridization, washing, and staining were conducted with the GeneChip® Hybridization, Wash and Stain Kit according to the manufacturer's guidelines. Arrays were scanned using the GeneChip® Scanner 3000, and raw data were acquired with Command Console Software 3.1 using default settings. Three biological replicates were included for each time point.

Microarray data analysis

The Bioinformatics Center at the Academy of Biological Sciences, Jilin University, performed gene screening and bioinformatic analysis. Differentially expressed genes were identified using a random-variance

model (RVM)-corrected analysis of variance (ANOVA). Significant profiles demonstrated a higher probability than expected by Fisher's exact test and multiple comparison tests. GO analysis was used to determine the main functions of the differentially expressed genes, based on the key functional classification of the National Center for Biotechnology Information (NCBI).

Real-time quantitative polymerase chain reaction assay

The collected nerve segments were preserved in RNA Stabilization Reagent (Qiagen, Hilden, Germany). Total RNA was extracted from the stored tissues using the RNeasy Mini Kit (Qiagen, Hilden, Germany) according to the manufacturer's protocol. Complementary DNA (cDNA) was synthesized from total RNA using the PrimeScript™ RT reagent Kit (TaKaRa, Dalian, China) following the manufacturer's instructions. RT-qPCR was performed using SYBR® Green Premix Ex Taq™ (TaKaRa) on an Applied Biosystems StepOne Real-Time PCR System. Relative messenger RNA (mRNA) expression levels were calculated using the comparative Ct (ΔΔCt) method and normalized to GAPDH mRNA expression at each time point. All reactions were run in triplicate, with data presented as the mean ± standard deviation (SD). The primers used for real-time qPCR are listed in Table 1. The thermocycling conditions were as follows: initial denaturation at 95°C for 30 s; 40 cycles of 95°C for 5 s, and 60°C for 30 s; followed by a melt curve analysis at 95°C for 15 s, 60°C for 60 s, and 90°C for 15 s.

Western blot analysis

Tissue samples were snap-frozen and homogenized immediately in ice-cold radioimmunoprecipitation assay (RIPA) buffer supplemented with protease and phosphatase inhibitors. Total protein concentration was determined with the bicinchoninic acid (BCA) assay. Twenty to thirty micrograms of protein per lane were separated on 10% sodium dodecyl sulfate–polyacrylamide gel electrophoresis (SDS-PAGE) gels and transferred to polyvinylidene fluoride (PVDF) membranes. After blocking with 5% non-fat milk in tris-buffered saline with Tween 20 (TBST) for one hour at room temperature, the membranes were incubated overnight at 4°C with the following primary antibodies: mouse anti-Ugt8 monoclonal antibody (1:200), mouse anti-Ccl2 (MCP-1) monoclonal antibody (1:1000), rabbit anti-Nrg1 polyclonal antibody (1:500), and rabbit anti-Hmox1 polyclonal antibody (1:500). Following three 10-minute washes with TBST, the membranes were probed with horseradish peroxidase (HRP)-conjugated secondary antibodies (1:1000) for one hour at room temperature. The membranes were cut horizontally so that β-actin and target proteins could be detected on separate strips. To strip and re-probe membranes, Western Blot Antibody Stripping Solution (Epizyme) was applied for 20 minutes at room temperature, followed by TBST washing and re-blocking. Bands were visualized with chemiluminescence and scanned with a GS800 densitometer. Band intensities were quantified using ImageJ and normalized to the corresponding β-actin signal for each time point.

Statistical analysis

Differentially expressed genes were selected in a logical sequence according to the RVM-ANOVA. The expression model profiles were correlated with the actual or expected number of genes assigned to each model profile. Significant profiles demonstrated a higher probability than expected by Fisher's exact test and multiple comparison tests. All data were expressed as mean ± SD and analyzed by one-way ANOVA and Scheffe's *post hoc* test using SPSS 23.0 for Windows (IBM Corp., NY, USA). When $p<0.05$, results were considered statistically significant.

Table 1. Primers used in real-time quantitative polymerase chain reaction assays.

Gene name	Forward primer 5′-3′	Reverse primer 5′-3′	Product length
GAPDH	GCAAGTTCAACGGCACAG	CGCCAGTAGACTCCACGAC	141
Ugt8	CGAAGGACGCGCTATGAAGT	CGCTGGAGGCTGTAGTGATT	228
Ccl2	TAGCATCCACGTGCTGTCTC	CAGCCGACTCATTGGGATCA	94
Nrg1	TCTTTCAGCCGCTGCGTTA	CATCGGCTCACCTCCAGAAG	378
Hmox1	CTAAGACCGCCTTCCTGCTC	CTGAGTGTGAGGACCCATCG	220

GAPDH – glyceraldehyde phosphate dehydrogenase; Ugt8 – UDP glycosyltransferase 8; Ccl2 – C-C motif chemokine ligand 2; Nrg1 – neuregulin 1; Hmox1 – heme oxygenase-1 (decycling).

RESULTS

Changes in gene expression associated with biological processes during nerve regeneration

Differentially expressed genes were identified for each biological process using GO enrichment analysis in the Database for Annotation, Visualization, and Integrated Discovery (DAVID) online tool (Zhang et al., 2021). We analyzed six biological processes closely related to peripheral nerve injury and regeneration: cell proliferation, cell migration, cell apoptosis, axon guidance, axonogenesis, and myelination. Most of these biological processes showed a tendency of relative balance between upregulation and downregulation across the experiment.

Table 2 shows the number of differentially expressed genes during various biological processes in distal segments at each time point. Most biological processes showed both upregulation and downregulation; all genes increased over time, and the time each peaked varied.

Cell proliferation genes became active over time, reaching a peak at six days, then gradually declined, with the balance between upregulation and downregulation mirroring the overall trend. Cell migration also peaked at day six and remained relatively stable until the last time point, with upregulation continuously dominant. Meanwhile, apoptosis was clearly elevated by day six and continued to increase, peaking at the final time point, with slightly greater upregulation at most time points. The tendencies of axon guidance, axonogenesis, and myelination were homologous. There were no initial readings (0 days), but this increased over time and remained relatively stable towards the end of the experiment (15 and 20 days). It is worth noting that no upregulation or downregulation of axonogenesis or myelination was identified during DAVID analysis.

Table 3 presents the numerical values and trends for four genes (*Ugt8*, *Ccl2, Nrg1, Hmox1*) selected to illustrate the microarray data. *Ugt8* expression declined from day 0, reached its lowest point on day three, then gradually increased and peaked on day 20. *Ccl2* first peaked on day three, declined on day 10, and reached its second peak (the highest) on day 20. *Nrg1* expression gradually increased, reaching a peak at day 15, after which it decreased significantly. *Hmox1* expression reached its first peak at day three, then gradually decreased, and reached its second peak (the highest) at day 20.

Temporal changes in Ugt8, Ccl2, Nrg1, and Hmox1 expression

We selected four genes (*Ugt8*, *Ccl2*, *Nrg1*, and *Hmox1*) with distinct functions in regeneration after peripheral nerve injury to demonstrate the accuracy of gene chips through molecular biological techniques. These four genes correlate with nerve regeneration after injury and participate in regulating the microenvironment that promotes it by activating inflammatory factors (Consoni et al., 2024).

Expression levels from each time point were compared to day 0 and statistically analyzed. The RT-qP-

Table 2. Biological processes of differentially expressed genes in distal nerve segments of rats at 0, 3, 6, 10, 15, and 20 days after sciatic nerve injury.

Biological process	0 d	3 d	6 d	10 d	15 d	20 d
Cell proliferation	25	110	310	214	156	125
Positive regulation	12	63	190	137	75	68
Negative regulation	15	50	102	77	52	47
Cell migration	11	35	126	110	100	102
Positive regulation	6	15	46	48	47	45
Negative regulation	2	10	55	29	42	31
Cell apoptosis	35	85	165	156	217	278
Positive regulation	21	46	88	75	112	151
Negative regulation	13	44	126	96	78	108
Axon guidance	0	8	15	18	39	35
Positive regulation	0	5	8	9	23	20
Negative regulation	0	7	11	13	13	11
Axonogenesis	0	21	28	31	36	32
Myelination	0	11	22	27	64	66

Cell proliferation, cell migration, cell apoptosis, and axon guidance showed both positive and negative regulation, whereas axonogenesis and myelination showed none.

Table 3. Expression of UDP glycosyltransferase 8 (*Ugt8*), C-C motif chemokine ligand 2 (*Ccl2*), neuregulin 1 (*Nrg1*), and heme oxygenase-1 (*Hmox1*) from microarray data analysis of distal sciatic nerve stumps of rats after sciatic nerve injury. Signal: expression intensity.

Probe Set ID	Gene symbol	0 d Signal	3 d Signal	6 d Signal	10 d Signal	15 d Signal	20 d Signal
1368858	*Ugt8*	728.3	279.1	385.5	585.5	816.3	1753.9
1367973	*Ccl2*	785.1	7246.7	4308.8	2494.8	3156.7	8317.7
1369783	*Nrg1*	30.4	27.7	61.6	116.1	216.8	39.7
1370080	*Hmox1*	432.4	1490	925.7	784.5	690.4	1560

CR results were generally consistent with the gene expression trend observed in the microarray analysis. The trend of *Ugt8* showed an initial decrease then peaked at the end of the experiment (day 20; F-value=72.508) (Fig. 1A). *Nrg1* remained relatively active, reaching its peak in the middle and later stages of the experiment (day 15) then showing a downward trend (F-value=43.114) (Fig. 1C). The trends of *Ccl2* and *Hmox1* were similar, with both peaking early (day 3-6), then decreasing, before peaking again at the end of the experiment (day 20;) (Fig. 1B and 1D). The analysis yielded F-values of 272.300 for *Ccl2* and 83.310 for *Hmox1*.

Ugt8, Ccl2, Nrg1, and Hmox1 protein levels after sciatic nerve injury

To further confirm the microarray and RT-qPCR analysis, we performed Western blot analysis of Ugt8, Ccl2, Nrg1, and Hmox1 proteins (Wang et al., 2016; Zhao et al., 2022), using β-actin as an internal control. The images indicated that the expression was similar to the results of the microarray and RT-qPCR analysis (Fig. 2). Ugt8 initially decreased, then peaked at the end of the experiment (day 20; F-value=34.196) (Fig. 3A). Nrg1 remained relatively active, peaked at day 15, then showed a decreasing trend (Fig. 3C; F-value=39.658). Mean-

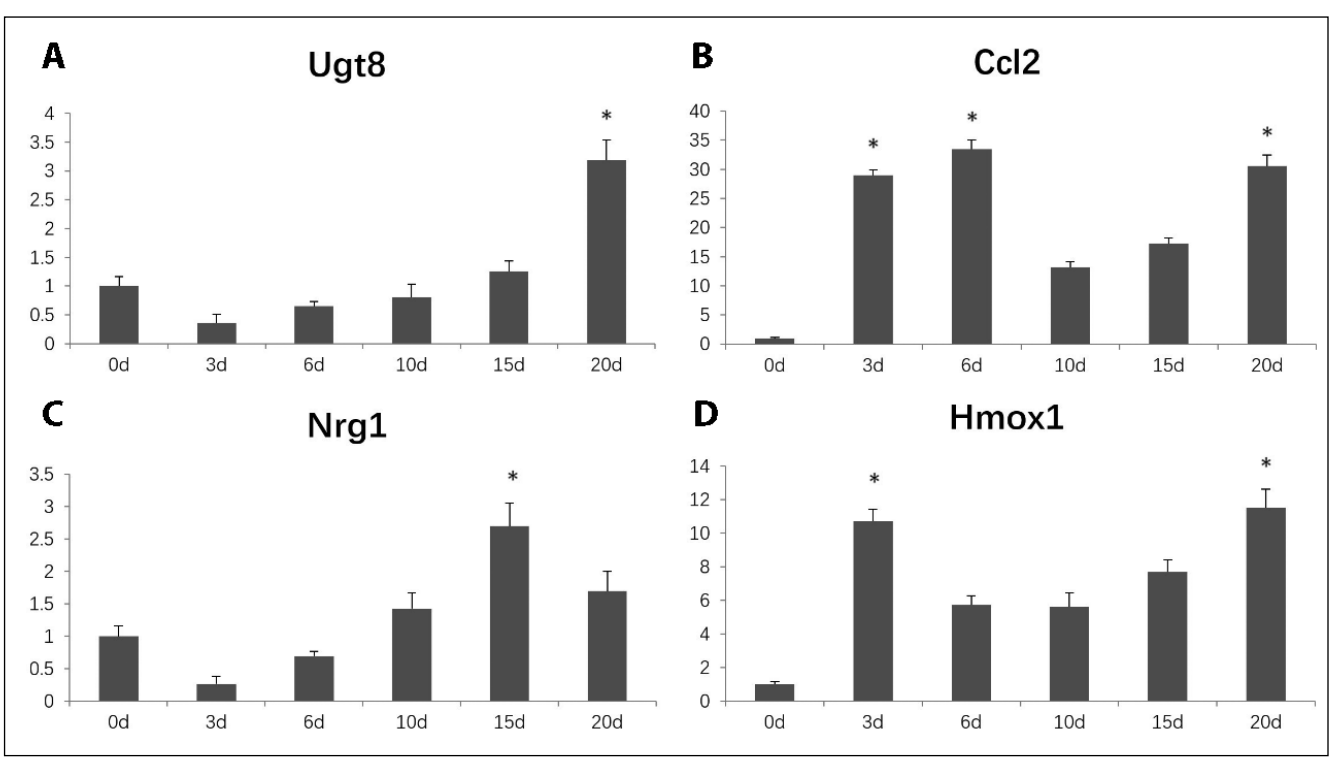

Fig. 1. Gene expression in rat distal sciatic nerve segments 0, 3, 6, 10, 15, and 20 days (d) after sciatic nerve injury (real-time quantitative polymerase chain reaction analysis). *P<0.05 *vs.* 0d. (A) UDP glycosyltransferase 8 (*Ugt8*) shows an initial decrease and then peaks at 20d. (B) C-C motif chemokine ligand 2 (*Ccl2*) peaked at 3-6d, and peaked again on 20d. (C) Neuregulin (*Nrg1*) peaked at 15d and then decreased. (D) Heme oxygenase-1 (*Hmox1*) peaked at 3d and again at 20d.

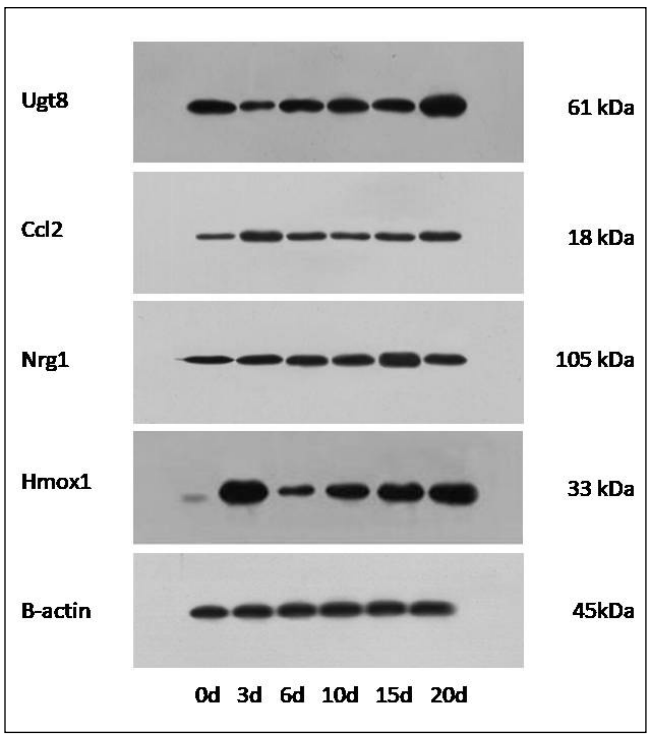

Fig. 2. Western blot analysis of total protein from distal sciatic nerve segments of rats at 0, 3, 6, 10, 15, and 20 days (d) after sciatic nerve injury.

while, Ccl2 and Hmox1 both peaked on day three, then decreased before peaking again on day 20 (Fig. 3B and 3D). The analysis yielded F-values of 49.000 for Ccl2 and 288.158 for Hmox1.

DISCUSSION

WD, a process that occurs before nerve regeneration, remains a subject of major interest in modern neurobiology. A large number of genes are differentially regulated during the distinct stages of WD, which are accompanied by a series of biological reactions and cellular interactions (Statello et al., 2021; Zhang et al., 2023). During regeneration after nerve injury, the injury triggers a switch in the genetic response, including a number of genes involved in both degeneration and regeneration (Goldman et al., 2020; Zhang et al., 2022). Therefore, we designed experiments to determine gene expression changes in the early period following peripheral nerve injury and identify the major biological processes during WD.

Cell proliferation, migration, and apoptosis underwent integral change, especially in the subacute phase (six days post-injury). Proliferation and migration

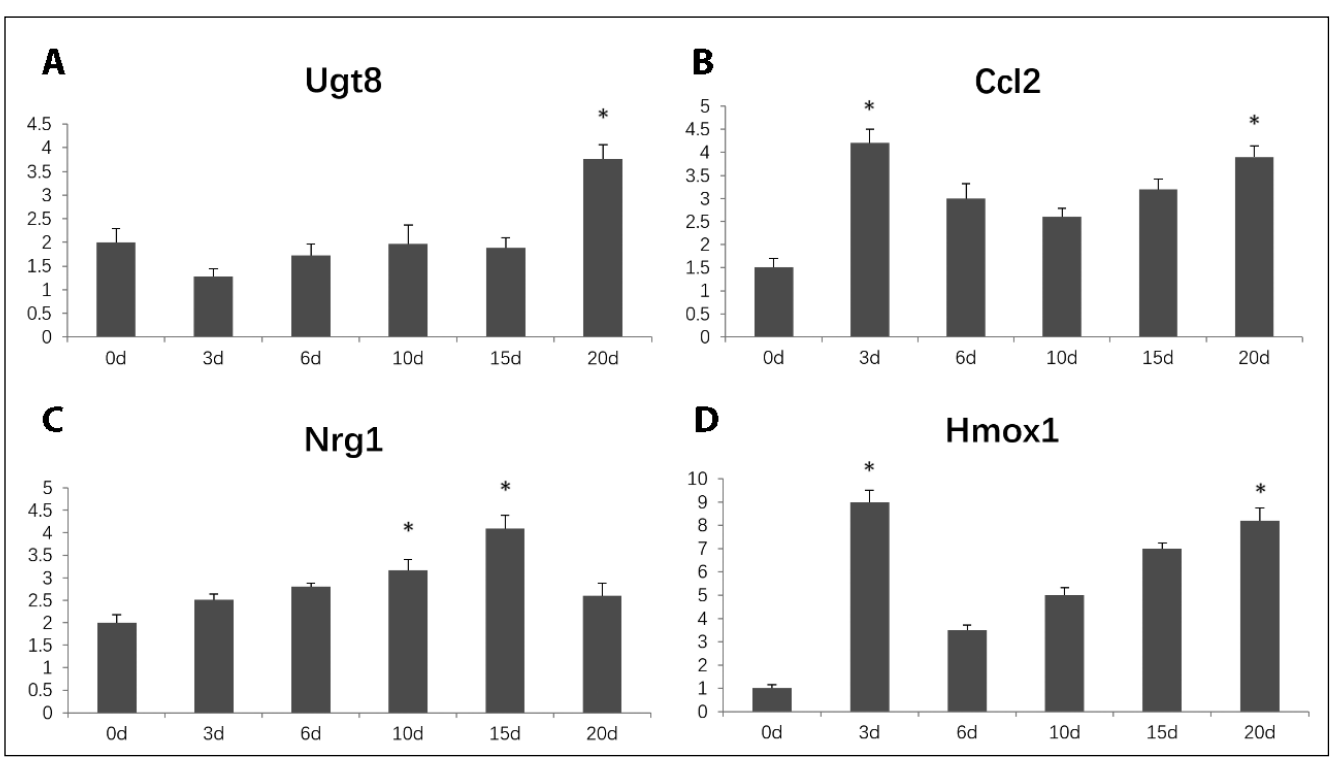

Fig. 3. Total protein expression from rat distal sciatic nerve segments after sciatic nerve injury. *P<0.05 *vs.* 0d. (A) UDP glycosyltransferase 8 (Ugt8) decreased initially and then peaked at 20d. (B) C-C motif chemokine ligand 2 (Ccl2) peaked at 3d and again at 20d. (C) Neuregulin (Nrg1) peaked at 15d then decreased. (D) Heme oxygenase-1 (Hmox1) peaked at 3d and again at 20d.

peaked before declining, though they remained active. In contrast, apoptosis remained elevated throughout. In the early stages after nerve transection, inflammatory and immune cells, such as neutrophils, lymphocytes, mononuclear cells, and macrophages, migrate to the injury site as initiating factors under the guidance of chemokines and proliferate to maintain immune responses. Therefore, the immune response, cell migration, and proliferation involved many identical differentially expressed genes (Merikangas et al., 2022). Despite a decrease in genes involved in the immune response, they increased in the later stages to clear cell debris and byproducts of inflammatory mediators.

Schwann cells require dedifferentiation and proliferation to form a Büngner's band, engulf debris, and create a favorable microenvironment for peripheral nerve regeneration; thus, cell proliferation maintains a consistent level (Jessen et al., 2022). Schwann cell apoptosis also occurs in the early stages of peripheral nerve degeneration, with both apoptosis and proliferation constituting a suitable microenvironment for the process. In our study, the results indicate that cell death downregulation was more dominant than upregulation six days after nerve transection. Substantial inflammation and immune cell migration occur at the injury site at this time, with proliferation maintaining these responses. However, the cell number remains relatively stable to avoid immune overreaction by maintaining a balance between proliferation, migration, and apoptosis. Our results show that apoptosis remained high in the latter stage, possibly due to the loss of innervation and the complete collapse of nerve cells. The results also indicate that the time course for nerve regeneration is not limited to three weeks.

Axonal guidance and axonogenesis remained active during the later stages of the experiment and represented a major phase of axon regeneration; thus, myelination exhibited a similar trend. During nerve regeneration, the growth cone, a specialized, motile, exploratory structure, forms at the tip of the regenerating axon. It is guided toward specific targets by the combined actions of attractive and repulsive guidance cues. Following sciatic nerve transection, axons undergo minor growth, but trigger axon guidance and axonogenesis (He et al., 2021). Myelin is essential for saltatory conduction of nerve signals in the peripheral nervous system. Following nerve injury, with the associated axonal damage and demyelination, demyelination enhances the extent of nerve regeneration (Hussain et al., 2020). Schwann cells undergo demyelination, dedifferentiation, and proliferation after peripheral nerve injury. After approximately one week, the regenerated axons are re-ensheathed and remyelinated by Schwann cells in the lesioned nerve (Ghezzi et al., 2023). In the current study, the number of differentially expressed genes involved in axon regeneration and myelination was relatively small. However, the genes involved in axon guidance and axonogenesis exhibited a similar change at the same time point (day 15), when peak expression occurred, suggesting that axon guidance and regeneration are interdependent. The gene expression related to myelination also showed a similar trend to the morphological characteristics. An explanation for the genes involved in myelination increasing without becoming numerous may be the poor function of their remyelination program.

To verify the microarray data obtained in our study, we analyzed four differentially expressed genes (*Ugt8*, *Ccl2*, *Nrg1*, and *Hmox1*) involved in nerve regeneration after injury. These genes are also involved in cytokine regulation, cell aggregation, and cell proliferation following nerve injury, as well as axon and myelin sheath formation during nerve regeneration.

The main function of *Ugt8* is to catalyze the formation of galactocerebroside, an important lipid component of the myelin sheath in the nervous system. Therefore, Ugt8 levels affect the stability and repair of the myelin sheath. Our research shows that Ugt8 expression decreased at the distal site following peripheral nerve injury, which is consistent with the process of myelin breakdown. In the later stages, expression significantly increased, facilitating myelin sheath regeneration.

Nrg1 promotes the proliferation and dedifferentiation of Schwann cells, the clearance of myelin sheaths, and axon regeneration. Our results show that Nrg1 levels decreased slightly in the early stage of injury, and Nrg1 is involved in the clearance of myelin fragments. In the later stage of repair, Nrg1 increased due to stimulation of Schwann cell dedifferentiation and proliferation, as well as axonal remyelination, reaching its peak within about two weeks.

Ccl2 can attract and activate monocytes/macrophages in the early stage after nerve injury, forming an inflammatory environment to clear myelin debris. In the later stage, due to myelin guidance and regeneration, and the activation of microglial cells, its expression reaches another peak around three weeks.

Hmox1 primarily regulates ferroptosis and influences immune cell polarization after peripheral nerve injury, with its expression significantly increased. In the early stage, it achieves high expression by promoting inflammatory responses and immune chemotaxis, then decreases. Due to the simultaneous occurrence of cellular apoptosis and proliferation, another peak in expression occurs around three weeks later.

Previous studies on the proximal segment of the injured sciatic nerve in rats have shown that the bio-

logical processes represented by genes were generally highly expressed from the early period (0.5-1 day) to the later period (≤14 days) (Li et al., 2013). Furthermore, some researchers have conducted studies on WD in the distal tissues of rat sciatic nerves after injury over a short time period (0-24 hours) (Yao et al., 2012). The studies mentioned analyzed gene expression in proximal and distal nerve segments at different time points after nerve injury, revealing distinct biological characteristics. Our research used the same time points and showed distinct expression patterns of biological characteristics, forming an effective complement. From our data, RT-qPCR and Western blot analysis showed the same trend as the gene microarray analysis, indicating that gene chips can be used to screen for key genes and biological processes.

The current study employed microarray technology to investigate gene expression patterns following peripheral nerve injury and identified trends in differentially expressed genes during critical phases of nerve regeneration. Our findings suggest that diverse biological processes are underpinned by a complex, dynamic regulatory network that involves highly influential genes within living organisms (Liu et al., 2020). In summary, examining the dynamic changes and biological roles of genes with varying expression levels will significantly enhance our understanding of the mechanisms driving peripheral nerve regeneration. We hope this study will help identify key regulatory genes involved in the regenerative process after peripheral nerve injury.

Nevertheless, this study has certain limitations. Specifically, our analysis does not fully address the initiators of the inflammatory and immune responses to injury, or the intricate signaling pathways and transduction mechanisms within the nerves themselves. Furthermore, while the GO enrichment analysis performed using DAVID provides useful insights, it is important to note that its results, in terms of the exact number of genes and the direction (positive or negative) of their regulatory effects, are indicative of trends rather than being absolute. Despite these limitations, our future work will focus on identifying key genes with the most pronounced changes in expression—both up- and down-regulated—that are likely to govern critical biological processes during peripheral nerve regeneration.

CONCLUSIONS

Our study employed gene chip analysis to identify differentially expressed genes in distal nerve segments during WD. We further analyzed the dynamic biological processes involving these genes and verified the findings using molecular biology techniques. This work provides a valuable foundation for screening key regulatory genes, offering insights for both basic research and clinical intervention strategies.

ACKNOWLEDGEMENTS

This work was supported by "Project of Health Talent of Jilin Province" (2019SCZ031).

REFERENCES

Bhunia, M. M., Stehn, C. M., Jubenville, T. A., Novacek, E. L., Larsson, A. T., Madala, M., Suppiah, S., Velez-Reyes, G. L., Williams, K. B., Sokolowski, M., Williams, R. L., Finnerty, S. J., Temiz, N. A., Caride, A., Bhagwate, A. V., Nagaraj, N. K., Lee, J. H., Ordog, T., Zadeh, G., & Largaespada, D. A. (2024). Multiomic analyses reveal new targets of polycomb repressor complex 2 in Schwann lineage cells and malignant peripheral nerve sheath tumors. *Neuro-oncology advances*, *6*(1), vdae188. https://doi.org/10.1093/noajnl/vdae188

Consonni, F. M., Incerti, M., Bertolotti, M., Ballerini, G., Garlatti, V., & Sica, A. (2024). Heme catabolism and heme oxygenase-1-expressing myeloid cells in pathophysiology. *Frontiers in immunology*, *15*, 1433113. https://doi.org/10.3389/fimmu.2024.1433113

Cooke, P., Janowitz, H., & Dougherty, S. E. (2022). Neuronal Redevelopment and the Regeneration of Neuromodulatory Axons in the Adult Mammalian Central Nervous System. *Frontiers in cellular neuroscience*, *16*, 872501. https://doi.org/10.3389/fncel.2022.872501

Costa-Silva, J., Domingues, D., & Lopes, F. M. (2017). RNA-Seq differential expression analysis: An extended review and a software tool. *PloS one*, *12*(12), e0190152. https://doi.org/10.1371/journal.pone.0190152

Dommel, S., & Blüher, M. (2021). Does C-C Motif Chemokine Ligand 2 (CCL2) Link Obesity to a Pro-Inflammatory State?. *International journal of molecular sciences*, *22*(3), 1500. https://doi.org/10.3390/ijms22031500

Fledrich, R., Kungl, T., Nave, K. A., & Stassart, R. M. (2019). Axo-glial interdependence in peripheral nerve development. *Development (Cambridge, England)*, *146*(21), dev151704. https://doi.org/10.1242/dev.151704

Ghezzi, L., Bollman, B., De Feo, L., Piccio, L., Trapp, B. D., Schmidt, R. E., & Cross, A. H. (2023). Schwann Cell Remyelination in the Multiple Sclerosis Central Nervous System. *Laboratory investigation; a journal of technical methods and pathology*, *103*(6), 100128. https://doi.org/10.1016/j.labinv.2023.100128

Goldman, J. A., & Poss, K. D. (2020). Gene regulatory programmes of tissue regeneration. *Nature reviews. Genetics*, *21*(9), 511–525. https://doi.org/10.1038/s41576-020-0239-7

Gong, L., Gu, Y., Han, X., Luan, C., Liu, C., Wang, X., Sun, Y., Zheng, M., Fang, M., Yang, S., Xu, L., Sun, H., Yu, B., Gu, X., & Zhou, S. (2023). Spatiotemporal Dynamics of the Molecular Expression Pattern and Intercellular Interactions in the Glial Scar Response to Spinal Cord Injury. *Neuroscience bulletin*, *39*(2), 213–244. https://doi.org/10.1007/s12264-022-00897-8

He, B., Pang, V., Liu, X., Xu, S., Zhang, Y., Djuanda, D., Wu, G., Xu, Y., & Zhu, Z. (2021). Interactions Among Nerve Regeneration, Angiogenesis, and the Immune Response Immediately After Sciatic Nerve Crush Injury in Sprague-Dawley Rats. *Frontiers in cellular neuroscience*, *15*, 717209. https://doi.org/10.3389/fncel.2021.717209

Hussain, G., Wang, J., Rasul, A., Anwar, H., Qasim, M., Zafar, S., Aziz, N., Razzaq, A., Hussain, R., de Aguilar, J. G., & Sun, T. (2020). Current Sta-

tus of Therapeutic Approaches against Peripheral Nerve Injuries: A Detailed Story from Injury to Recovery. *International journal of biological sciences*, *16*(1), 116–134. https://doi.org/10.7150/ijbs.35653

Jessen, K. R., & Mirsky, R. (2022). The Role of c-Jun and Autocrine Signaling Loops in the Control of Repair Schwann Cells and Regeneration. *Frontiers in cellular neuroscience*, *15*, 820216. https://doi.org/10.3389/fncel.2021.820216

Krishnan, A., Verge, V. M. K., & Zochodne, D. W. (2024). Hallmarks of peripheral nerve injury and regeneration. *Handbook of clinical neurology*, *201*, 1–17. https://doi.org/10.1016/B978-0-323-90108-6.00014-4

Li, R., Li, D. H., Zhang, H. Y., Wang, J., Li, X. K., & Xiao, J. (2020). Growth factors-based therapeutic strategies and their underlying signaling mechanisms for peripheral nerve regeneration. *Acta pharmacologica Sinica*, *41*(10), 1289–1300. https://doi.org/10.1038/s41401-019-0338-1

Li, S., Liu, Q., Wang, Y., Gu, Y., Liu, D., Wang, C., Ding, G., Chen, J., Liu, J., & Gu, X. (2013). Differential gene expression profiling and biological process analysis in proximal nerve segments after sciatic nerve transection. *PloS one*, *8*(2), e57000. https://doi.org/10.1371/journal.pone.0057000

Lin, Y. F., Xie, Z., Zhou, J., Yin, G., & Lin, H. D. (2019). Differential gene and protein expression between rat tibial nerve and common peroneal nerve during Wallerian degeneration. *Neural regeneration research*, *14*(12), 2183–2191. https://doi.org/10.4103/1673-5374.262602

Liu, M., Yao, B., Gui, T., Guo, C., Wu, X., Li, J., Ma, L., Deng, Y., Xu, P., Wang, Y., Yang, D., Li, Q., Zeng, X., Li, X., Hu, R., Ge, J., Yu, Z., Chen, Y., Chen, B., Ju, J., Zhao, Q. (2020). PRMT5-dependent transcriptional repression of c-Myc target genes promotes gastric cancer progression. *Theranostics*, *10*(10), 4437–4452. https://doi.org/10.7150/thno.42047

Merikangas, A. K., Shelly, M., Knighton, A., Kotler, N., Tanenbaum, N., & Almasy, L. (2022). What genes are differentially expressed in individuals with schizophrenia? A systematic review. *Molecular psychiatry*, *27*(3), 1373–1383. https://doi.org/10.1038/s41380-021-01420-7

Mietto, B. S., Mostacada, K., & Martinez, A. M. (2015). Neurotrauma and inflammation: CNS and PNS responses. *Mediators of inflammation*, *2015*, 251204. https://doi.org/10.1155/2015/251204

Seyednasrollah, F., Laiho, A., & Elo, L. L. (2015). Comparison of software packages for detecting differential expression in RNA-seq studies. *Briefings in bioinformatics*, *16*(1), 59–70. https://doi.org/10.1093/bib/bbt086

Sobrido-Camean, D., & Barreiro-Iglesias, A. (2022). Morpholino studies shed light on the signaling pathways regulating axon regeneration in lampreys. *Neural regeneration research*, *17*(7), 1475–1477. https://doi.org/10.4103/1673-5374.330597

Statello, L., Guo, C. J., Chen, L. L., & Huarte, M. (2021). Gene regulation by long non-coding RNAs and its biological functions. *Nature reviews. Molecular cell biology*, *22*(2), 96–118. https://doi.org/10.1038/s41580-020-00315-9

Thamizhoviya, G., & Vanisree, A. J. (2021). Enriched Environment Enhances the Myelin Regulatory Factor by mTOR Signaling and Protects the Myelin Membrane Against Oxidative Damage in Rats Exposed to Chronic Immobilization Stress. *Neurochemical research*, *46*(12), 3314–3324. https://doi.org/10.1007/s11064-021-03433-8

Wang, Y., Guo, Z. Y., Sun, X., Lu, S. B., Xu, W. J., Zhao, Q., & Peng, J. (2016). Identification of Changes in Gene expression of rats after Sensory and Motor Nerves Injury. *Scientific reports*, *6*, 26579. https://doi.org/10.1038/srep26579

Wang, Y., Wei, J., Zhang, P., Zhang, X., Wang, Y., Chen, W., Zhao, Y., & Cui, X. (2022). Neuregulin-1, a potential therapeutic target for cardiac repair. *Frontiers in pharmacology*, *13*, 945206. https://doi.org/10.3389/fphar.2022.945206

Yao, D., Li, M., Shen, D., Ding, F., Lu, S., Zhao, Q., & Gu, X. (2012). Gene expression profiling of the rat sciatic nerve in early Wallerian degeneration after injury. *Neural regeneration research*, *7*(17), 1285–1292. https://doi.org/10.3969/j.issn.1673-5374.2012.17.001

Yao, D., Li, M., Shen, D., Ding, F., Lu, S., Zhao, Q., & Gu, X. (2013). Expression changes and bioinformatic analysis of Wallerian degeneration after sciatic nerve injury in rat. *Neuroscience bulletin*, *29*(3), 321–332. https://doi.org/10.1007/s12264-013-1340-0

Zhang, Y., Qazi, S., & Raza, K. (2021). Differential expression analysis in ovarian cancer: A functional genomics and systems biology approach. *Saudi journal of biological sciences*, *28*(7), 4069–4081. https://doi.org/10.1016/j.sjbs.2021.04.022

Zhang, C., Talifu, Z., Xu, X., Liu, W., Ke, H., Pan, Y., Li, Y., Bai, F., Jing, Y., Li, Z., Li, Z., Yang, D., Gao, F., Du, L., Li, J., & Yu, Y. (2023). MicroRNAs in spinal cord injury: A narrative review. *Frontiers in molecular neuroscience*, *16*, 1099256. https://doi.org/10.3389/fnmol.2023.1099256

Zhang, Y., Xu, L., Li, X., Chen, Z., Chen, J., Zhang, T., Gu, X., & Yang, J. (2022). Deciphering the dynamic niches and regeneration-associated transcriptional program of motoneurons following peripheral nerve injury. *iScience*, *25*(9), 104917. https://doi.org/10.1016/j.isci.2022.104917

Zhang, Z., Yu, D., Seo, M., Hersh, C. P., Weiss, S. T., & Qiu, W. (2019). Novel Data Transformations for RNA-seq Differential Expression Analysis. *Scientific reports*, *9*(1), 4820. https://doi.org/10.1038/s41598-019-41315-w

Zhao, X. F., Huffman, L. D., Hafner, H., Athaiya, M., Finneran, M. C., Kalinski, A. L., Kohen, R., Flynn, C., Passino, R., Johnson, C. N., Kohrman, D., Kawaguchi, R., Yang, L. J. S., Twiss, J. L., Geschwind, D. H., Corfas, G., & Giger, R. J. (2022). The injured sciatic nerve atlas (iSNAT), insights into the cellular and molecular basis of neural tissue degeneration and regeneration. *eLife*, *11*, e80881. https://doi.org/10.7554/eLife.80881